

# Saccular Limited Dorsal Myeloschisis with Spinal Cord Deviation out of the Spinal Canal to the Sac

Ai KUROGI,<sup>1</sup> Takato MORIOKA,<sup>2</sup> Nobuya MURAKAMI,<sup>1</sup> Takafumi SHIMOGAWA,<sup>3</sup> Nobutaka MUKAE,<sup>3</sup> Yoshihiro MATSUO,<sup>4</sup> Naoyuki IMAMOTO,<sup>4</sup> Yuki TATEISHI,<sup>5</sup> and Satoshi O. SUZUKI<sup>6</sup>

<sup>1</sup>Department of Neurosurgery, Fukuoka Children's Hospital, Fukuoka, Fukuoka, Japan

<sup>2</sup>Department of Neurosurgery, Harasanshin Hospital, Fukuoka, Fukuoka, Japan

<sup>3</sup>Department of Neurosurgery, Graduate School of Medical Sciences, Kyushu University, Fukuoka, Fukuoka, Japan

<sup>4</sup>Department of Neurosurgery, Japan Community Health Care Organization (JCHO), Kyushu Hospital, Kitakyushu, Fukuoka, Japan

<sup>5</sup>Department of Pathology, Japan Community Health Care Organization (JCHO), Kyushu Hospital, Kitakyushu, Fukuoka, Japan

<sup>6</sup>Department of Psychiatry, Shourai Hospital, Karatsu, Saga, Japan

## Abstract

Saccular limited dorsal myeloschisis (LDM) is characterized by a fibroneural stalk linking the saccular skin lesion to the underlying spinal cord. Since untethering surgery during the early postnatal period is often indicated to prevent sac rupture, saccular LDM should be distinguished from myelomeningocele (MMC) during the perinatal period. We treated two patients with the spinal cord deviation from the spinal canal to the sac, which mimicked a prolapse of the neural placode into the MMC sac. In patient 1, pre- and postnatal magnetic resonance imaging (MRI) revealed that the spinal cord was strongly tethered to the thick stalk. During surgery, the dorsally bent cord and stalk were united, and the border between these two was determined with intraoperative neurophysiological mapping (IONM). In patient 2, the spinal cord was tethered to two slender stalks close to each other, which was visible with the combined use of sagittal and axial postnatal three-dimensional heavily T2-weighted imaging (3D-hT2WI). The preoperative MRI hallmark of saccular LDM is the visualization of a stalk that links the bending cord and sac. Complete untethering surgery to return the cord into the spinal canal and correct its dorsal bending is recommended.

Keywords: endodermal cyst, glial fibrillary acidic protein, half-Fourier acquisition, single-shot turbo spin-echo sequence

## Introduction

The term limited dorsal myeloschisis (LDM) was first described as a distinct clinicopathological entity of spinal dysraphism by Pang et al.<sup>1–4</sup> LDM is thought to originate from a small segmental failure of the dorsal closure of the neural folds during

primary neurulation. At the focal limited non-closure site, the disjunction between the cutaneous and neural ectoderms is impaired. This results in a retained fibroneural stalk linking the skin lesion and the dorsal spinal cord, which results in the tethering of the cord.<sup>1–4</sup> The recommended treatment consists of a prophylactic untethering of the stalk from the cord.<sup>1–4</sup>

Based on the skin manifestation, LDMs were originally categorized as saccular and non-saccular (flat).<sup>1,2</sup> Saccular LDM consists of a skin-based cerebrospinal fluid (CSF) sac topped by a squamous epithelial dome, whereas the flat LDM has a

Received June 3, 2021; Accepted August 19, 2021

Copyright© 2021 The Japan Neurosurgical Society  
This work is licensed under a Creative Commons Attribution-NonCommercial-NoDerivatives International License.

squamous epithelial flat surface or a sunken crater or pit typically called a “cigarette-burn” skin lesion.<sup>1–6</sup> Recently, we reported a human tail-like cutaneous appendage as an additional morphological type of skin lesion.<sup>7–10</sup> Between April 2015 and December 2020, 23 Japanese LDM patients underwent initial untethering surgery at our hospitals. The external skin lesions were flat in 13 patients, sacular in 5, and tail-like in 5.

The preoperative diagnosis could be made based on the presence of the stalk that connects the skin lesions and the dorsal spinal cord on magnetic resonance image (MRI).<sup>1–4</sup> However, in infants with slender stalk, it is often difficult to diagnose with MRI.<sup>4–6,11</sup> Although the central histopathological feature of an LDM stalk is the presence of a glial fibrillary acidic protein (GFAP)-immunopositive neuroglial tissue in the fibrocollagenous stalk, a hallmark of the stalk’s origin from the non-dysjunctioned neuroectoderm,<sup>1–4</sup> immunopositivity for GFAP was observed in approximately 50% of pathologically examined cases.<sup>4–6</sup> Thus, the clinical diagnosis of LDM should be based on comprehensive analysis of clinical, neuroradiological, operative, and histopathological findings.<sup>4–6</sup>

For the sacular LDM, untethering surgery during the early postnatal period is often indicated, unlike for flat and tail-like LDM, because it prevents rupture of the sac or a major hindrance to proper handling of the baby.<sup>1–6,11–13</sup> Therefore, sacular LDM should be distinguished from open spinal dysraphism centered on a myelomeningocele (MMC) during the perinatal period.<sup>11,13–15</sup> MMCs generally have poor functional outcome; however, LDMs can have good outcomes with appropriate untethering surgery.<sup>1–3,11,13–15</sup> Among the five sacular LDMs, two patients had spinal cord deviation from the spinal canal to the sac, probably due to the fairly strong tethering effect, which mimicked a prolapse of the neural placode into the MMC sac. We, herein, describe these cases and discuss the diagnostic and surgical strategies.

## Case Reports

### Patient 1

A 19-year-old primigravida was referred to us at 32<sup>+2</sup> weeks of gestation, following the detection of a CSF-filled mass in the lumbar region on ultrasound (US) examination. Prenatal MRI at 33<sup>+3</sup> weeks, including half-Fourier acquisition single-shot turbo spin-echo sequence (HASTE) image, demonstrated severe dorsal bending and deviation of the cord to the sac out of the spinal canal due to the tethering effect of the thick stalk attached to the sac. The spinal cord bent approximately at right angles and ran dorsally to attach to the inner wall of the sac

before running ventrally back into the spinal canal (Fig. 1a). However, the bending cord and stalk were united and the boundary was not determined. No hydrocephalus or Chiari malformation was observed.

The baby boy weighing 2760 g was delivered, with Apgar scores of 8 and 8, via a scheduled cesarean section at 37<sup>+3</sup> weeks. Physical examination revealed a dorsal midline sac measuring 42 × 35 mm in the upper lumbar region, which was torn during delivery (Fig. 1b). He had no neurological deficits. Postnatal MRI examination, including three-dimensional heavily T2-weighted imaging (3D-hT2WI) confirmed a severe dorsal bending and deviation of the cord to the sac, and out of the spinal canal, at the L1-L2 vertebral level (Fig. 1c) while the sac was collapsed. The bending cord and stalk were united, similar to the findings of prenatal MRI.

On the next day after birth, untethering and repair surgery for the sac were performed. Opening the sac with a widening of the tear, a thick stalk and tethered cord, which measured 8–9 mm in diameter and 15 mm in length together, emerged from the orifice of the spinal canal and attached to the wall of the sac (Fig. 1d, e-1). A skin erosion was noted on the outer surface of the sac where the stalk was attached. The border between the spinal cord and stalk could not be distinguished, and nerve root-like structures were found near the orifice of the spinal canal (Fig. 1e-2). This border was neurophysiologically determined by tracing the evoked compound muscle action potentials (CMAPs) of the external anal sphincter muscle, hamstring, and gastrocnemius with direct bipolar stimulation with 2 mA intensity starting from the functional cord and continuing to the non-functional stalk. The CMAPs were evoked following stimulation at 0–5 mm from the orifice of the spinal canal; no CMAPs were evoked following stimulation at 10 mm or more peripheral from the orifice (Fig. 1f). The stalk was severed at 10 mm from the orifice. The cut edge was approximated with a pial suture and returned to the spinal canal. Due to the small size of the orifice, the anatomical relationship between the cord and stalk was not determined.

Postoperatively, *de novo* neurological abnormalities were not observed. MRI performed on the postoperative 25th day demonstrated that the dorsal bending of the cord markedly improved due to the successful untethering of the cord, although 5 mm of the stalk persisted (Fig. 1g). Hydromyelic central canal distended the remnant stalk. Histopathologically, the resected stalk included a fibrocollagenous tissue embedded with GFAP-immunopositive neuroglial tissues (Fig. 1h and 1i). The sac was covered with finely jagged squamous epithelium, except for the attachment of the stalk.

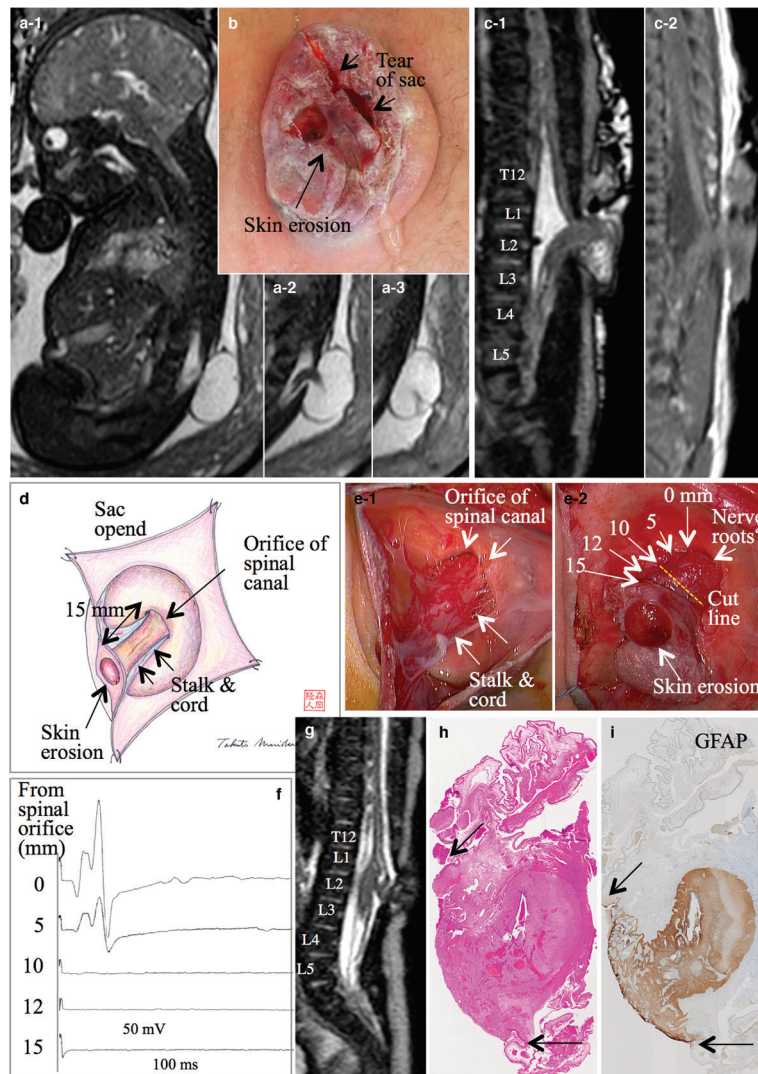


**Fig. 1** (Patient 1). (a) Serial upside-down sagittal views of HASTE sequence (slice thickness 3 mm) performed at 33<sup>+3</sup> weeks of gestation show severe dorsal bending of the cord and deviation to the sac out of the spinal canal. No hydrocephalus or Chiari malformation is observed. (b) Photograph at birth showing a saccular lesion at the upper lumbar region. A cleft and skin erosion are noted on the surface. (c) Sagittal views of 3D-hT2WI (slice thickness, 0.45 mm) (c-1) and variable flip-angle 3D-T1WI (slice thickness, 0.45 mm) (c-2) at birth confirm that the cord shows severe dorsal bending and deviation to the sac out of the spinal canal at the L1-L2 vertebral level while the sac is collapsed. (d, e, f) Schematic drawing (d) and microscopic view of the intraoperative findings (e), and IONM (f). (d, e-1) Opening the sac, a thick stalk and tethered cord, measuring 15 mm in length together, emerge from the orifice of the spinal canal and attaches to the inner wall of the sac. (e-2) A skin erosion is observed on the outer surface of the sac where the stalk is attached. The border between spinal cord and the stalk cannot be distinguished, whereas nerve root-like structures are found near the orifice of the spinal canal. This border is neurophysiologically determined by tracing the evoked CMAPs of the hamstring with direct stimulation with 2 mA intensity starting from the functional cord and continuing to the non-functional stalk (f). CMAPs are obtained following stimulation at 0–5 mm from the orifice of spinal canal; no CMAPs are evoked following the distal stimulation at 10 mm or more. The stalk is severed at 10 mm from the orifice. Numbers indicated in e-2 and f represent the distance (mm) from the orifice of the cord. (g) Sagittal view of 3D-hT2WI (slice thickness, 0.45 mm), performed on postoperative 25th day, demonstrates marked improvement in dorsal bending of the cord, although 5.3 mm of the stalk persists. (h, i) Histopathologically, the resected stalk includes a fibrocollagenous tissue embedded with GFAP-immunopositive neuroglial tissues. The sac is covered with finely jagged squamous epithelium, except for the attachment of stalk (black arrows). Original magnification  $\times 12.5$ . 3D-T1WI: three-dimensional turbo spin-echo T1-weighted images, 3D-hT2WI: three-dimensional heavily T2-weighted imaging, CMAPs: compound muscle action potentials, GFAP: glial fibrillary acidic protein, HASTE: half-Fourier acquisition single-shot turbo spin-echo, IONM: intraoperative neurophysiological mapping.

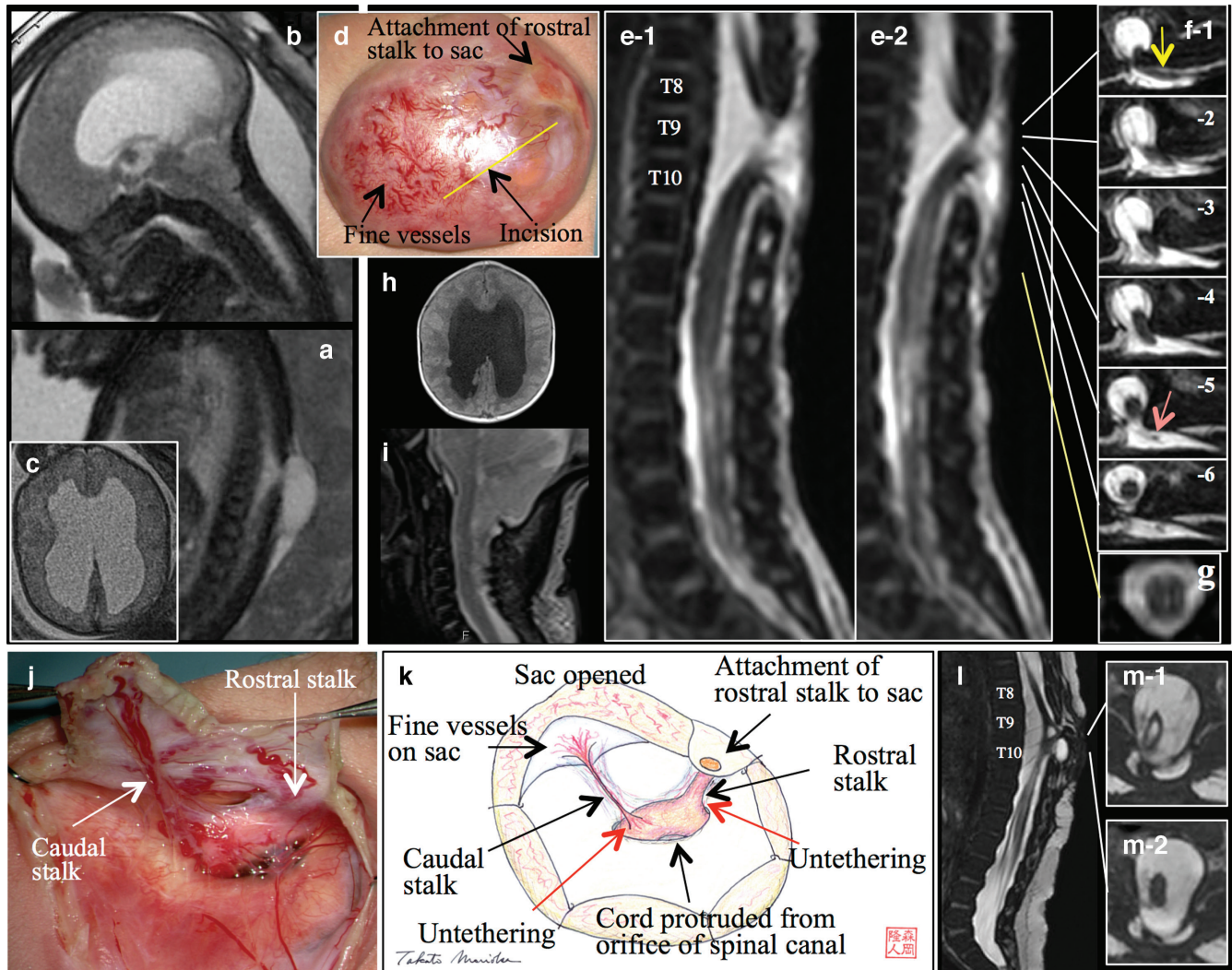


**Fig. 2** (Patient 2). (a) Sagittal view of HASTE image (slice thickness 5 mm) performed at 31<sup>+1</sup> weeks of gestation shows a dorsal tenting of the spinal subarachnoid space continuous with the sac, but it fails to reveal the exact anatomical relationship involving the cord, stalk and sac. Sagittal (b) and axial images (c) of cranial HASTE images (slice thickness 5 mm) show hydrocephalus and Chiari malformation. (d) Photograph showing a sacular skin lesion at the lower thoracic region. (e) Serial sagittal images of 3D-hT2WI (slice thickness 1.25 mm) demonstrates a severe dorsal bending and deviation of the lumbar cord to the sac out of the spinal canal at the T8-T10 vertebral level but does not reveal the stalk. (f) Serial axial images of 3D-hT2WI (slice thickness 1.25 mm) show that the stalk is attached to the rostral part of the sac (f-1, yellow arrow) and the tethered cord deviates to the sac (f-2, 3, 4). The existence of another slender stalk is suspected (f-5, red arrow) and the caudal cord returns to the spinal canal. (g) Axial view of T2WI (slice thickness 4 mm) shows a narrow slit, indicating a type II SCM, at the caudal cord to the dorsally bending site. Axial T1-weighted image of the head (slice thickness 4 mm) (h) and sagittal T2WI of the craniocervical junction (slice thickness 3 mm) (i) show ventriculomegaly with subependymal nodular heterotopias on both sides and Chiari malformation, respectively. (j, k) Microscopic view (j) and schematic drawing of the intraoperative findings (k). Opening the sac shows two stalks linking between the cord, protruding from the orifice of the spinal canal, and inner wall of the sac, are observed. Each stalk is severed at the attachment with the cord, and the cord is returned to the spinal canal. (l, m) Sagittal (l) and serial axial views of 3D-hT2WI (slice thickness 1.25 mm), performed on postoperative 39th day, demonstrate that the cord has been returned to the spinal canal with the successful untethering surgery. The dorsal bending of the cord improves to some extent, but it persists. Hydromyelic central canal is observed at the attachment of the stalk. Epidural fluid collection is observed. 3D-hT2WI: three-dimensional heavily T2-weighted imaging, HASTE: half-Fourier acquisition single-shot turbo spin-echo, SCM: split cord malformation, T2WI: T2-weighted image.

During the patient's 11-month postoperative follow-up, his development was normal, without neurological deficits.

### Patient 2

A 32-year-old, gravida 3, para 2 woman was referred to us at 29<sup>+2</sup> weeks of gestation, following the detection of a CSF-filled mass in the lower thoracic region, ventriculomegaly, and Chiari malformation on US examination. Prenatal MRI at 31<sup>+1</sup> weeks did not reveal the anatomical relationship involving the cord, stalk, and sac, although the dorsal tenting of the subarachnoid space continuous with the sac was demonstrated (Fig. 2a). Hydrocephalus and Chiari malformation were also observed (Fig. 2b and 2c).

At 37<sup>+2</sup> weeks, labor was pharmacologically induced because of planned delivery. The mother vaginally delivered a male neonate weighing 2882 g with Apgar scores of 9 and 9. Physical examination revealed a dorsal midline sac measuring 42 × 33 mm, with small blood vessels on the surface at the lower thoracic level (Fig. 2d). He had no neurological deficit. Sagittal 3D-hT2WI images showed severe dorsal bending and deviation of the spinal cord to the sac out of the spinal canal at the T8–T10 vertebral levels, but it did not show the stalk (Fig. 2e). Serial axial 3D-hT2WI images demonstrated that the stalk was attached to the rostral part of the sac (Fig. 2f-1) and the tethered cord deviated to the sac (Fig. 2f-2, 3, 4). The existence of another slender stalk was suspected (Fig. 2f-5), and the caudal cord returned to the spinal canal (Fig. 2f-4, 5, 6). Type II split cord malformation (SCM) was observed at the caudal cord to the dorsally bending site (Fig. 2g). Cranial MRI showed ventriculomegaly with subependymal nodular heterotopias on the both sides (Fig. 2h) and Chiari malformation (Fig. 2i).

On the next day after birth, following the placement of Ommaya's reservoir, untethering and repair surgery for the sac were performed. Opening the sac (Fig. 2d), two stalks linking the bending cord, protruding from the orifice of the spinal canal, and inner wall of the sac were observed after dissecting the surrounding connective tissue (Fig. 2j and k). The rostral and caudal stalk had the following diameters; 1.6–2.0 mm and 0.4–0.8 mm, respectively. Each stalk was severed at the attachment with the cord, and the cord was returned to the spinal canal.

Postoperatively, *de novo* neurological abnormalities were not observed. MRI performed on the postoperative 39th day demonstrated that the cord returned to the spinal canal after successful untethering surgery (Fig. 2l, m-1, 2). The dorsal bending of the cord improved to an extent, but it persisted. The hydromyelic central canal was observed at the

stalk attachment. Ommaya's reservoir was replaced by a ventriculoperitoneal shunt on the postoperative 77th day.

Histopathologically, the rostral stalk included a fibrocollagenous tissue embedded with GFAP-immunopositive neuroglial tissues (Fig. 3a) containing several neurons (Fig. 3b). The attachment of the rostral stalk to the sac had a partial ependymal lining and was densely infiltrated with neutrophils (Fig. 3c). The caudal stalk also included a fibrocollagenous tissue embedded with GFAP-immunopositive neuroglial tissues, an endodermal cyst lined by bronchial epithelium (Fig. 3d), peripheral nerve bundles, and arachnoid villi-like structures (Fig. 3e). The sac to which the caudal stalk attached was covered by keratinizing stratified squamous epithelium with angiomatous dilated blood vessels (Fig. 3f).

During the patient's 10-month postoperative follow-up, his development was normal, without neurological deficits.

## Discussion

According to the original description by Pang et al,<sup>1,2</sup> some LDM stalks are stout, and their tethering effects on the spinal cord are obvious. The tension in the stalk is illustrated by a dorsally tented thecal sac at the point of dural penetration, and the cord is also tented dorsally at the stalk-cord union. However, there are no reports of cases with the spinal cord deviations from the spinal canal into the sac. In this report, the spinal cord was strongly tethered to a thick stalk in patient 1 and two slender stalks that were close to each other in patient 2.

The prenatal imaging hallmark of saccular LDM is the visualization of a stalk that links the cord and sac,<sup>11,14,15</sup> while that of MMC is the presence of neural placode in the sac continuous from the cord.<sup>16–19</sup> Although prenatal MRI sequences such as HASTE or fast imaging with steady precession allow the acquisition of diagnostic images within a reasonably short time, their shortcoming is the necessity to increase the slice thickness.<sup>11,19</sup> The 3- to 5-mm-thick sections obtained by prenatal MRI in the present study provided sufficient image of the thick stalk in patient 1 and the prenatal diagnosis of LDM was possible; however, the details of the slender stalks in patient 2 were insufficient.<sup>11</sup> Complication of hydrocephalus and Chiari malformation are common in patients with MMC<sup>16–19</sup> but rare in those with LDM.<sup>11</sup> However, the complications of these pathologies on prenatal MRI do not deny the diagnosis of LDM, as demonstrated in patient 2 who had subependymal nodular heterotopias in addition to these anomalies.

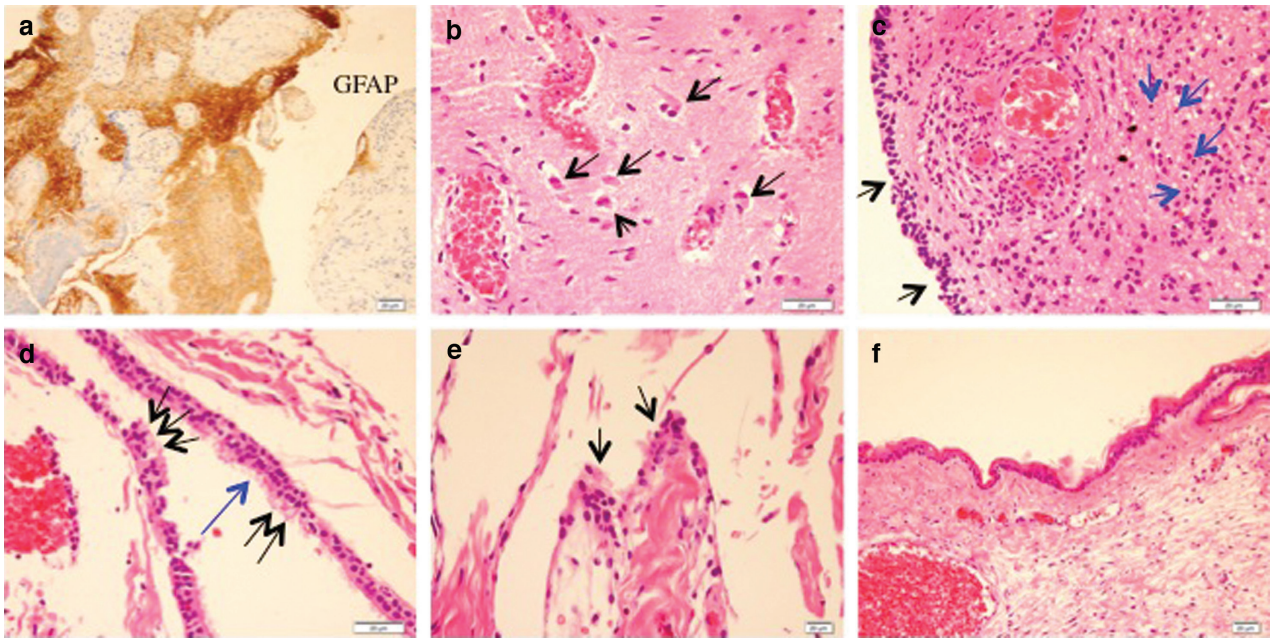


**Fig. 3 (Patient 2).** Histopathological findings of the rostral (a, b, c) and caudal stalks (d, e, f). (a) The rostral stalk includes a fibrocollagenous tissue embedded with GFAP-immunopositive neuroglial tissues (a) containing several neurons (b, black arrows). The attachment of the rostral stalk to the sac has a partial ependymal lining (black arrows in c) and it is densely infiltrated with neutrophils (blue arrows in c). The caudal stalk has an endodermal cyst lined by bronchial epithelium, including goblet cells (black arrows in d), and ciliated columnar epithelial cells (blue arrow in d) and arachnoid villi-like structures (black arrow in e). The sac to which the caudal stalk attached is covered by keratinizing stratified squamous epithelium with angiomas dilated blood vessels (3f). Scale bars indicate 20  $\mu\text{m}$ . GFAP: glial fibrillary acidic protein.

We previously reported the utility of postnatal 3D-hT2WI in demonstrating a slender stalk in saccular LDM patients.<sup>5,11,12</sup> However, we could not observe the two slender stalks on sagittal 3D-hT2WI for patient 2. This is probably because 1.25-mm-thick sections in the present study are still insufficient to demonstrate the details of a slender stalk, which could be overcome with the additional use of axial 3D-hT2WI,<sup>5,11</sup> as was demonstrated in patient 2. Thus, the postnatal diagnosis of LDM was possible in patient 2.

Since the diagnosis of LDM was made based on the preoperative MRI (prenatal MRI in patient 1 and postnatal MRI in patient 2), the primary purpose of surgery was cord untethering. During surgery, it is recommended to sever the LDM stalk at the cord attachment and resect the entire length of the stalk,<sup>1-4,20,21</sup> which could be performed in patient 2. However, in patient 1, we could not morphologically distinguish the border between dorsally bended cord and the LDM stalk under an operative microscope, and this border was determined by intraoperative neurophysiological mapping (IONM). However, postoperative MRI demonstrated that the cord-stalk attachment was located 5 mm farther to the central

side. To prevent the current spread through the CSF during IONM, which could result in false-positive findings, we ensured that the operative field was dry. We think that it could not be completely prevented because the tissue itself contains water.

Another purpose of untethering surgery in these two patients is to return the cord into the spinal canal and correct its severe dorsal bending. Although the former purpose was achieved in both cases, the latter purpose has not been fully achieved in patient 2. The cause is not clear, but it may involve physiological kyphosis of the thoracic spine. Since both of the remnant thick stalk in patient 1 and the dorsal bending of the cord in patient 2 may cause the re-tethered cord syndrome,<sup>22</sup> close observation with repeated MRI is needed.

Another noteworthy finding on postoperative MRI was the development of syringomyelia immediately rostral to the stalk-cord attachment. The caudal pole of the syrinx extended to the stalk at the attachment instead of the caudal cord. This finding was consistent with our previous report and further supported the idea that herniation of the hydromyelic central canal to the stalk is a possible pathological mechanism underlying syringomyelia

development.<sup>12)</sup> Since the natural course of LDM-associated syringomyelia is still unknown,<sup>8,12)</sup> close observation is also important in this regard.

All of the stalks in patient 1 and two stalks in patient 2 had GFAP-immunopositive neuroglial tissues in the fibrocollagenous stalk, which is a typical histopathological finding of LDM.<sup>1-6)</sup> In patient 2, the attachment of the rostral stalk to the sac had a partial ependymal lining. This finding may support the idea that segmental myelocystocele is involved in the development of saccular LDM.<sup>1-4,12)</sup>

A notable histopathological finding of the caudal stalk in patient 2 was the presence of endodermal (neurenteric) cyst. The development of the endodermal cyst may be involved in the type II SCM in patient 2, as demonstrated by previous authors, including us.<sup>1,2,5)</sup> The embryogenesis is thought to involve dorsally displaced endodermal stem cells through the reminiscent of the ventrodorsal endomesenchymal tract that traverses the entire embryonic plate from the amniotic cavity to the yolk sac.<sup>23,24)</sup>

### Acknowledgments

We thank Dr. Tadahisa Shono, Department of Neurosurgery, Harasanshin Hospital for supporting our study. We thank Editage for editing a draft of this manuscript.

### Statement of Ethics

Written informed consent was obtained from the parents of the children for the publication of this case report

### Funding

This work was partly supported by the Research Foundation of Fukuoka Children's Hospital.

### Authors' Contribution

Kurogi A, Morioka T, Murakami N, and Suzuki SO: Study design and project outline. Kurogi A, Takafumi Shimogawa, Nobutaka Mukae, Matsuo Y, Imamoto N, and Tateishi Y: Data acquisition, analysis, and manuscript drafting. Morioka T, Murakami N, and Suzuki SO: Critical revision of the manuscript and figures.

### Conflicts of Interest Disclosure

The authors declare that they have no conflicts of interest.

### References

- 1) Pang D, Zovickian J, Oviedo A, Moes GS: Limited dorsal myeloschisis: a distinctive clinicopathological entity. *Neurosurgery* 67: 1555–1579; discussion 1579–1580, 2010
- 2) Pang D, Zovickian J, Wong ST, Hou YJ, Moes GS: Limited dorsal myeloschisis: a not-so-rare form of primary neurulation defect. *Childs Nerv Syst* 29: 1459–1484, 2013
- 3) Wong ST, Kan A, Pang D: Limited dorsal spinal nondisjunctional disorders: limited dorsal myeloschisis, congenital spinal dermal sinus tract, and mixed lesions. In: Di Rocco C, Pang D, Rutka JT (eds). *Textbook of Pediatric Neurosurgery*. 1st Edition. Switzerland: Springer, 2010. 10.1007/978-3-319-31512-6\_110-1.
- 4) Morioka T, Murakami N, Mukae N, et al.: Surgical pathoembryology and treatment of limited dorsal myeloschisis. *Jpn J Neurosurg (Tokyo)* 30: 424–431, 2021 (Japanese)
- 5) Morioka T, Suzuki SO, Murakami N, et al.: Neurosurgical pathology of limited dorsal myeloschisis. *Childs Nerv Syst* 34: 293–303, 2018
- 6) Morioka T, Suzuki SO, Murakami N, et al.: Surgical histopathology of limited dorsal myeloschisis with flat skin lesion. *Childs Nerv Syst* 35: 119–128, 2019
- 7) Abe K, Mukae N, Morioka T, Shimogawa T, Suzuki SO, Mizoguchi M: Tail-like cutaneous appendage at the upper thoracic region with a continuous stalk of limited dorsal myeloschisis. *Interdiscip Neurosurg* 22: 100823, 2020
- 8) Morioka T, Murakami N, Ichiyama M, Kusuda T, Suzuki SO: Congenital dermal sinus elements in each tethering stalk of coexisting thoracic limited dorsal myeloschisis and retained medullary cord. *Pediatr Neurosurg* 55: 380–387, 2020
- 9) Murakami N, Morioka T, Suzuki SO, et al.: Clinicopathological findings of limited dorsal myeloschisis associated with spinal lipoma of dorsal-type. *Interdiscip Neurosurg* 21: 100781, 2020
- 10) Sarukawa M, Morioka T, Murakami N, et al.: Human tail-like cutaneous appendage with a contiguous stalk of limited dorsal myeloschisis. *Childs Nerv Syst* 35: 973–978, 2019
- 11) Tomita Y, Morioka T, Murakami N, Noguchi Y, Sato Y, Suzuki SO: Slender stalk with combined features of saccular limited dorsal myeloschisis and congenital dermal sinus in a neonate. *Pediatr Neurosurg* 54: 125–131, 2019
- 12) Morioka T, Murakami N, Yanagida H, et al.: Terminal syringomyelia associated with lumbar limited dorsal myeloschisis. *Childs Nerv Syst* 36: 819–826, 2020
- 13) Russell NE, Chalouhi GE, DiRocco F, Zerah M, Ville Y: Not all large neural tube defects have a poor prognosis: a case of prenatally diagnosed limited dorsal myeloschisis. *Ultrasound Obstet Gynecol* 42: 238–239, 2013

- 14) Friszer S, Dhombres F, Morel B, Zerah M, Jouannic JM, Garel C: Limited dorsal myeloschisis: a diagnostic pitfall in the prenatal ultrasound of fetal dysraphism. *Fetal Diagn Ther* 41: 136–144, 2017
- 15) Lafitte AS, Blouet M, Belloy F, Borha A, Benoist G: A case of prenatally diagnosed limited dorsal myeloschisis with good prognosis. *J Clin Ultrasound* 46: 282–285, 2018
- 16) Morioka T, Hashiguchi K, Mukae N, Sayama T, Sasaki T: Neurosurgical management of patients with lumbosacral myeloschisis. *Neurol Med Chir (Tokyo)* 50: 870–876, 2010
- 17) Murakami N, Morioka T, Hashiguchi K, et al.: Usefulness of three-dimensional T1-weighted spoiled gradient-recalled echo and three-dimensional heavily T2-weighted images in preoperative evaluation of spinal dysraphism. *Childs Nerv Syst* 29: 1905–1914, 2013
- 18) Hashiguchi K, Morioka T, Yoshida F, et al.: Feasibility and limitation of constructive interference in steady-state (CISS) MR imaging in neonates with lumbosacral myeloschisis. *Neuroradiology* 49: 579–585, 2007
- 19) Hashiguchi K, Morioka T, Murakami N, et al.: Clinical significance of prenatal and postnatal heavily T2-weighted magnetic resonance images in patients with myelomeningocele. *Pediatr Neurosurg* 50: 310–320, 2015
- 20) Eibach S, Moes G, Zovickian J, Pang D: Limited dorsal myeloschisis associated with dermoid elements. *Childs Nerv Syst* 33: 55–67, 2017
- 21) Lee JY, Chong S, Choi YH, et al.: Modification of surgical procedure for “probable” limited dorsal myeloschisis. *J Neurosurg Pediatr* 19: 616–619, 2017
- 22) Chatterjee S, Rao KS: Missed limited dorsal myeloschisis: an unfortunate cause for recurrent tethered cord syndrome. *Childs Nerv Syst* 31: 1553–1557, 2015
- 23) Muthkumar N, Arunthathi J, Sunder V: Split cord malformation and neureteric cyst-case report and a theory of embryogenesis. *Br J Neurosurg* 14: 488–492, 2000
- 24) Pang D, Dias MS, Ahab-Barmada M: Split cord malformation: part I: a unified theory of embryogenesis for double spinal cord malformations. *Neurosurgery* 31: 451–480, 1992

---

Corresponding author: Ai Kurogi, MD  
 Department of Neurosurgery, Fukuoka Children's Hospital, 5-1-1 Kashiiteriha, Higashi-ku, Fukuoka, Fukuoka 813-0017, Japan.  
*e-mail*: aironron8282@gmail.com